

ligands form bonds with Ru(II) that are shorter than the distance found in $[(\text{NH}_3)_5\text{RuMepz}]^{3+}$. In $[(\text{NH}_3)_5\text{Ru}_2\text{N}_2](\text{BF}_4)_4$, the Ru-N(dinitrogen) bond length is 1.928 (6) Å.²⁰ The Ru-N(nitrosyl) distance in $[(\text{NH}_3)_5\text{RuNO}]\text{Cl}_3 \cdot \text{H}_2\text{O}$ is 1.770 (9) Å.²¹ The Ru-N(nitro) distance in $[(\text{NH}_3)_5\text{RuNO}_2]\text{Cl} \cdot \text{H}_2\text{O}$ is 1.906 (5) Å.¹⁴

The shrinking of the Ru-N(Mepz) bond when Ru(III) is reduced has implications for the reactivity of the couple as a redox reagent, and it is of interest to estimate the magnitude of the effect. A major cause of the difference in the self-exchange rates for the $\text{Fe}(\text{H}_2\text{O})^{3+/2+}$ and $\text{Ru}(\text{NH}_3)^{3+/2+}$ couples is the difference in the inner-sphere reorganization energies, estimated by Sutin²² as 8.4 kcal/mol for the former couple and 0.9 for the latter. In this connection it is of interest to learn what the effect of the shortening of the Ru-N(Mepz) bond on reducing Ru(III) to Ru(II) on the self-exchange rate is expected to be. Calculations using for the present case $\Delta r = -0.13$ and 0.03 Å for the Ru-N(Mepz) and Ru-N(NH₃) bonds, respectively, on reduction and the assumption made by Sutin for the force constants yielded an inner-sphere reorganization energy of 1.6 kcal. In view of the difference in charge type (4+/3+ in the present case compared to 3+/2+), it would be difficult to trace the effect on this particular structural parameter on the rates of electron transfer for the couple.

Acknowledgment. Support of this work by a National Science Foundation Graduate Fellowship for J.F.W. is gratefully acknowledged.

Registry No. II, 103026-88-6; III, 103026-90-0; $[(\text{NH}_3)_5\text{RuMepz}](\text{ClO}_4)_3$, 41557-35-1.

Supplementary Material Available: Listings of thermal parameters for both structures and tables of bond distances and angles for the anions in compound III (6 pages). Ordering information is given on any current masthead page.

- (20) Treitel, I. M.; Flood, M. T.; Marsh, R. E.; Gray, H. B. *J. Am. Chem. Soc.* **1969**, *91*, 6512.
 (21) Bottomley, F. *J. Chem. Soc., Dalton Trans.* **1974**, 1600.
 (22) Sutin, N. In *Tunneling in Biological Systems*; Chance, B., DeVault, D. C., Frauenfelder, H.; Marcus, R. A., Schrieffer, J. R., Sutin, N., Eds.; Academic: New York, 1979; pp 201-227.

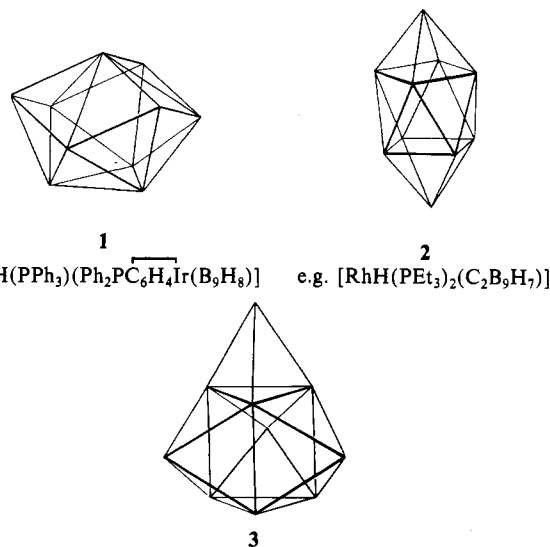
Contribution from the Inorganic Chemistry Laboratory,
University of Oxford, Oxford OX1 3QR, U.K.

Molecular Orbital Calculations Relevant to the Hyper-Closo vs. Iso-Closo Controversy in Metallaboranes

Roy L. Johnston and D. Michael P. Mingos*

Received April 25, 1986

Greenwood, Kennedy and their co-workers¹ have recently described some interesting metallaboranes whose polyhedral structures are not those normally found for nine- and ten-vertex closo-metallaboranes. An example of such a ten-vertex metallaborane is illustrated in **1** and contrasted with the more usual bicapped square-antiprismatic geometry (**2**).² Since both **1** and **2** have triangular faces exclusively, Greenwood et al. have suggested that **1** is an isomeric form of **2** and recommended that it and related structures be described as iso-closo.^{3,4} Baker⁵ has



noted that if the metal fragment in **1** contributes its usual number of electrons for skeletal bonding then **1** has one fewer skeletal electron pairs than **2** and suggested that **1** represents an example of a new class of hyper-closo polyhedra with n rather than $n + 1$ skeletal electron pairs. Baker⁵ has proposed that the capping principle⁶ can be adapted to account for the electron deficiency in **1**, although, as Kennedy has noted,⁷ **1** is geometrically quite distinct from the capped closo structure **3** anticipated from the capping rules. Kennedy has surmised that if the metal contributes four orbitals to skeletal bonding rather than the three generally assumed in simple electron-counting rules,⁸ then it is not unreasonable for high-connectivity clusters such as **1** to be expected.

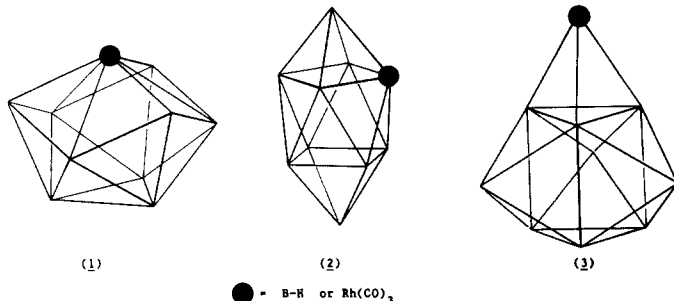
In this paper we now describe some molecular orbital calculations and a theoretical analysis based on Stone's tensor surface harmonic theory⁹⁻¹¹ that resolve this controversy.

In Table I the computed total energies for $\text{B}_{10}\text{H}_{10}$ and the metallaborane $\text{B}_9\text{H}_9\text{M}(\text{CO})_3$ ¹² are presented for idealized geometries based on 1-3 and electron counts corresponding to the presence of 10 and 11 skeletal electron pairs. Even for the boranes the calculations provide a clear geometric distinction: the bicapped square-antiprismatic geometry (**2**) is the favored geometry for $n + 1$ skeletal electron pairs, and **1** is favored for n skeletal electron pairs. The tetracapped trigonal prism (**3**) is also characterized by n bonding skeletal electron pairs, in accordance with the capping principle,⁶ but is less stable than **1** and **2** for both electron counts. The s and p valence orbitals of boron do not lead to effective overlaps for a boron atom above a triangular face and therefore such capped structures are generally unfavorable for borane polyhedra.¹³

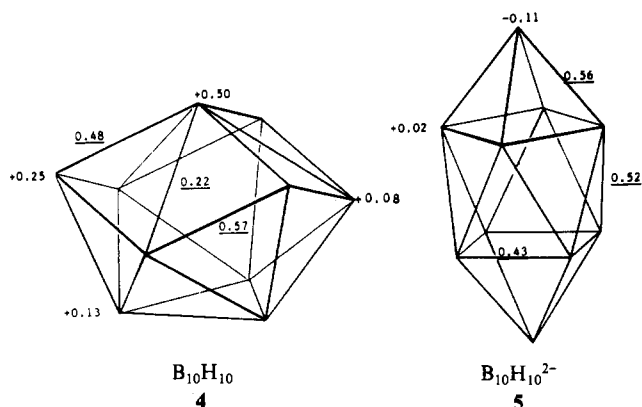
The different number of bonding molecular orbitals in **1** and **2** is not accidental but reflects an important and general topological distinction in deltahedral boranes, which can be interpreted by using Stone's tensor surface harmonic theory. For spherical deltahedral borane clusters that belong to the S_{4m} and D_{md} point groups, the tangential p^* orbitals give rise to a symmetric distribution of nL^* bonding and nL^* antibonding molecular orbitals. In contrast spherical clusters belonging to the C_{mv} point groups

- (1) Greenwood, N. N. *Pure Appl. Chem.* **1983**, *55*, 77-87, 1415-1430.
 (2) Barker, G. K.; Garcia, M. P.; Green, M.; Stone, F. G. A.; Bassett, J. M.; Welch, A. J. *J. Chem. Soc., Chem. Commun.* **1981**, 653-655.
 (3) Bould, J.; Greenwood, N. N.; Kennedy, J. D.; McDonald, W. S. *J. Chem. Soc., Chem. Commun.* **1982**, 465-467.
 (4) Bould, J.; Crook, J. E.; Greenwood, N. N.; Kennedy, J. D.; McDonald, W. S. *J. Chem. Soc., Chem. Commun.* **1982**, 346-348.

- (5) Baker, R. T. *Inorg. Chem.* **1986**, *25*, 109-111.
 (6) Mingos, D. M. P.; Forsyth, M. I. *J. Chem. Soc., Dalton Trans.* **1977**, 610-616.
 (7) Kennedy, J. D. *Inorg. Chem.* **1986**, *25*, 111-112.
 (8) Mingos, D. M. P. *Acc. Chem. Res.* **1984**, *17*, 311-319.
 (9) Stone, A. J. *Mol. Phys.* **1980**, *41*, 1339-1354.
 (10) Stone, A. J. *Inorg. Chem.* **1981**, *20*, 563-571.
 (11) Stone, A. J. *Polyhedron* **1984**, *3*, 1299-1308.
 (12) For a description of the extended Hückel molecular orbital calculations used in this paper see: Mingos, D. M. P. *J. Chem. Soc., Dalton Trans.* **1977**, 602-610. The B, C, H, and O parameters are described in this paper. For Rh the H_{ii} parameters are -12.50 (4d), -8.09 (5s), and -4.57 (5p) eV. The cluster geometries were based on B-B = 1.70 Å, Rh-C = 1.80 Å, C-O = 1.10 Å, and Rh-B = 2.17 and 2.40 Å.
 (13) Jemmis, E. D. *J. Am. Chem. Soc.* **1982**, *104*, 7017-7020.

Table I. Sum of One-Electron Energies for Polar (1), Spherical (2), and Capped (3) Deltahedral Clusters with 10 Vertices (eV)


$B_{10}H_{10}$	-602.80	-601.62	-600.06	10 skeletal \bar{s} pairs
$B_{10}H_{10}^{2-}$	-620.23	-621.29	-614.40	11 skeletal \bar{s} pairs
$[Rh(CO)_3B_9H_9]^+$	-1256.25	-1254.55	-1249.02	10 skeletal \bar{s} pairs
$[Rh(CO)_3B_9H_9]^-$	-1273.45	-1273.77	-1266.94	11 skeletal \bar{s} pairs

Chart I. Computed Charges and Overlap Populations (Underlined>

($m \geq 3$) and having an odd number of atoms lying on the C_m axis have $(n-1)L^\pi$ bonding, $(n-1)L^*$ antibonding, and a pair of L^π/L^* nonbonding molecular orbitals (see Figure 1 for a specific illustration of the molecular orbitals for **1** and **2**). Therefore, for spherical borane clusters a change in electron count from $(n+1)$ to n can lead to a change in skeletal geometry that interconverts the deltahedron into an alternative deltahedron belonging to a C_{mv} point group. Topologically this transformation interconverts a *spherical deltahedron* (with a symmetrical distribution of vertices with the same valencies) into a *polar deltahedron* (with a unique vertex of high connectivity on the principal rotation axis). Similar conclusions based on a group theoretical analysis have been derived for high-nuclearity ($n \geq 12$) borane polyhedra by Fowler.¹⁴

The computed charge and overlap populations for $B_{10}H_{10}$ with the polar deltahedral geometry **1** show large variations (see **4** and **5** in Chart I, for example), which arise from the presence of a boron atom of high connectivity. The *spherical* to *polar* transformation is therefore resisted by these charge separation effects in B_nH_n and B_nCl_n polyhedral molecules. However, the large positive charge on the axial boron atom and the lower overlap populations for bonds radiating from this atom suggest that the *polar* skeletal geometry is further stabilized by the introduction of a metal atom at this site. The computed energies for the metallaboranes $[Rh(CO)_3B_9H_9]^+$ or $[Rh(CO)_3B_9H_9]^-$ (see Table I) confirm that although the conventional deltahedral geometry is preferred for the case with $(n+1)$ skeletal electron pairs, the C_{3v} polar deltahedron is substantially more stable for n skeletal electron pairs.

These particular calculations provide no support for Kennedy's surmise that the ML_3 fragment in the polar deltahedron (**1**) could contribute an extra orbital for skeletal bonding. An analysis of

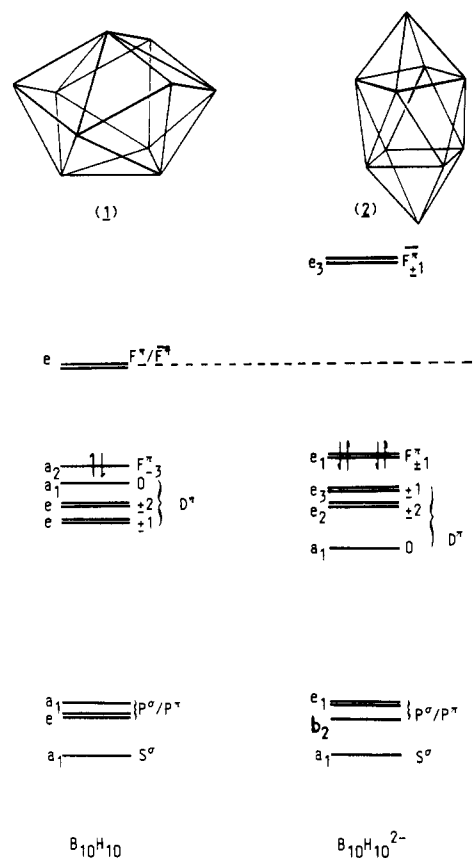


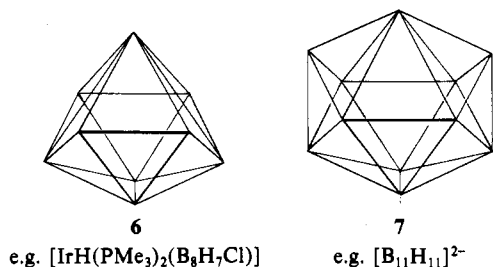
Figure 1. Schematic representations of the molecular orbitals for $B_{10}H_{10}$ with the skeletal geometries **1** and **2**. Symmetries and Stone tensor surface harmonic labels are given to each of the molecular orbitals. For the polar deltahedral cluster some mixing with functions of higher L quantum numbers occurs; e.g. D_0^* has admixtures of F_0^* . The highest occupied orbitals in the clusters are indicated by pairs of antiparallel arrows.

the computed overlap populations and overlap integrals has shown that the bonding occurs primarily through the metal d_{xz} and d_{yz} orbitals with little contribution from $d_{x^2-y^2}$ and d_{xy} . Furthermore, the relative contributions of these orbitals to the bonding in the polar and spherical deltahedra are very similar. Indeed on pure symmetry grounds the C_{3v} symmetry of **1** dictates that either both or neither of the $d_{x^2-y^2}$, d_{xy} pair be involved in bonding. The calculations suggest that their limited bonding effects are canceled by four-electron-destabilizing interactions.

In summary the calculations support in general terms the hyper-closo- model proposed by Baker and have revealed a topo-

(14) Fowler, P. W. *Polyhedron* **1985**, *4*, 2051-2057.

logical transformation for generating polar deltahedra with n skeletal electron pairs. The symmetry restrictions arising from the definition of polar deltahedra with a unique atom on the principle axis limits them to clusters with $3p + 1$ atoms belonging to the C_{3v} and T_d point groups. The tetrahedron ($p = 1$) and capped octahedron ($p = 2$) represent other examples of polar deltahedral clusters with n bonding skeletal electron pairs. Fowler¹⁴ has identified polyhedra with 16, 19, and 22 atoms that belong to the C_{3v} and T_d point groups and have n skeletal electron pairs. For deltahedra with C_{2v} symmetry, e.g. 6 and 7 the de-



generacy of the L^*/L^* nonbonding set is no longer dictated by the symmetry and whether they have n or $n + 1$ skeletal electron pairs is influenced by the extent to which the degeneracy is removed. In $B_9H_9^{2-}$ and $B_{11}H_{11}^{2-}$ the degeneracy is removed sufficiently for $n + 1$ skeletal electron pairs to be accommodated. For $B_{13}H_{13}$ Fowler's calculations suggest that the degeneracy is retained sufficiently for the n electron pair situation to be preferred.¹⁴ The introduction of a metal fragment on the principal axis in 6 and 7 could, however, lead to a stabilization of the n electron pair situation. Baker⁷ has cited some examples of such compounds in his paper.

Acknowledgment. The SERC is thanked for financial support, and M. Walters is thanked for developing a graphics program for representing the polyhedral structures.

—————

Contribution from the Chemistry Division, Naval Research
Laboratory, Washington, D.C. 20375-5000,
and Department of Chemistry, University of Massachusetts,
Amherst, Massachusetts 01003

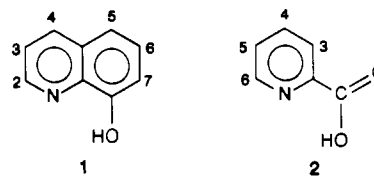
Tungsten(IV/V) Eight-Coordinate Mixed-Ligand-Chelate Electrochemistry

Robert J. Nowak^{1a} and Ronald D. Archer*^{1b}

Received July 1, 1985

Quantitative cyclic voltammetric measurements on the complete series of eight-coordinate tungsten chelates of the general formula $ML_nL'_{4-n}$ where $n = 0-4$ indicate a smooth change in $E^{o'}$ from 0.404 to 0.275 V for $L = 5,7$ -dichloroquinolinolato and $L' = 5$ -methylpicolinato in tetrahydrofuran vs. a sodium-saturated calomel electrode. The change parallels the MLCT spectral transition change although the magnitude of the redox change is a little lower than that of the charge-transfer transition. Together these two series of values provide information as to the relative energies of the HOMO and LUMO levels of such eight-coordinate systems.

Inert, completely chelated eight-coordinate complexes of tungsten can be prepared through the reaction of excess 8-quinolinol (Hq, 1) and picolinic acid (Hpic, 2) derivatives with a variety of tungsten compounds at elevated temperatures,² even



though the chemistry of tungsten with classical Werner type ligands is dominated by oxo species such as $WO_2(q)_2$.³ The very stable d² tungsten(IV) $W(q)_4$ and $W(pic)_4$ type species are 18-electron complexes. Even so, they can be oxidized to the analogous tungsten(V) 17-electron $W(q)_4^+$ and $W(pic)_4^+$ type species, also thought to be 8-coordinate.⁴ Oxidation occurs spontaneously at elevated temperatures in the presence of excess ligand or at room temperature with chlorine, bromine, or perchloric acid. The tungsten(V) chelates disproportionate in strong base, such as alcoholic KOH, to give $W(q)_4$ and $WO_2(q)_2$ type complexes, or they undergo reduction cleanly to $W(q)_4$ with copper metal.⁴ However, no quantitative electrochemical data have been available to correlate the relative oxidation-reduction tendencies of the quinolinato and picolinato chelates. The lack of electrochemical data is not surprising given the extremely low solubility of $W(q)_4$ in all practical electrochemical solvents. However, the availability of an entire series of $W(dcq)_n(mplic)_{4-n}$ chelates (where $n = 0-4$, Hdcq = 5,7-dichloro-8-quinolinol, and Hmpic = 5-methylpicolinic acid),⁵ which have better solubility, makes such a study feasible and is the subject of this paper.

Cyano and dithio type ligands, such as dithio acids, dithiocarbamates, and dithioxanthates, also stabilize tungsten in these two oxidation states via eight-coordination. The electrochemical data available on these other systems show a wide variation in the relative stability of the two oxidation states.⁶

The stability and inertness of the eight-coordinate tungsten(IV) and -(V) chelates has been explained in terms of π -overlap in several of the papers noted above by using an extension of the original suggestion of Orgel.⁷ Ligand exchange is very slow, and even isomer rearrangements have high activation parameters.⁵ Proof of eight-coordination with a geometry consistent with Orgel's rule has been obtained through a crystal structure of one of the tungsten(IV) chelates.⁸ The electronic spectra of all of the tungsten(IV) quinolinolates and picolinates have low energy (ca. 14 000-17 000 cm^{-1}) metal-to-ligand charge-transfer transitions^{2,5} and the analogous tungsten(V) ions exhibit ligand-to-metal charge-transfer bands in the visible region.⁴ The determination of electrochemical properties of these species allows further elucidation of these inert chelates.

Experimental Section

Syntheses. The tungsten chelates were synthesized by using procedures reported previously: $W(dcq)_4$ and $W(mplic)_4$ were prepared from $W(CO)_6$ and excess ligand at elevated temperature.² The mixed-ligand species $W(dcq)_3(mplic)$, $W(dcq)_2(mplic)_2$, and $W(dcq)(mpic)_3$ were prepared similarly by using ligand mixtures and were purified by chromatography on silica gel.⁵ Purity was ascertained by elemental analysis and proton NMR and electronic spectra; cf. ref 5.

Electrochemical Measurements. The lithium perchlorate (Eastman) electrolyte was stored in a vacuum oven at 50 °C for several weeks before use. The solvent, tetrahydrofuran (Burdick and Jackson UV grade), was heated under reflux conditions over calcium hydride and then distilled under an inert atmosphere. Platinum electrodes (Bioanalytical Systems, W. Lafayette, IN) were polished on a Buehler high-speed polishing wheel. Metadi diamond paste (0.25 μm) was used for the final polishing. Electrodes were sonicated in ASTM type I or better water followed by THF to remove traces of polishing compound. An electrochemical cell

(1) (a) Naval Research Laboratory. (b) University of Massachusetts.
(2) Donahue, C. J.; Archer, R. D. *Inorg. Chem.* 1977, 16, 2903. Dorset, T. E.; Walton, R. A. *J. Chem. Soc., Dalton Trans.* 1976, 347. Bonds, W. D., Jr.; Archer, R. D. *Inorg. Chem.* 1971, 10, 2057. Archer, R. D.; Bonds, W. D., Jr. *J. Am. Chem. Soc.* 1967, 89, 2236.

(3) Rice, C. A.; Spence, J. T.; Kroneda, M. H. *Inorg. Chem.* 1981, 20, 1996.
(4) Bonds, W. D., Jr.; Archer, R. D.; Pribush, R. A. *Inorg. Chem.* 1972, 11, 1550.
(5) Donahue, C. J.; Archer, R. D. *J. Am. Chem. Soc.* 1977, 99, 6613.
(6) Nieuwpoort, A.; Steggerda, J. J. *Recl. Trav. Chim. Pays-Bas* 1976, 95, 250.
(7) Orgel, L. E. *J. Inorg. Nucl. Chem.* 1960, 14, 135.
(8) Bonds, W. D., Jr.; Archer, R. D.; Hamilton, W. C. *Inorg. Chem.* 1971, 10, 1764.